ELSEVIER

Cardiovascular Research 57 (2003) 1062–1071

Cardiovascular Research

www.elsevier.com/locate/cardiores

What happens when cardiac Na channel function is compromised? 2. Numerical studies of the vulnerable period in tissue altered by drugs

C. Frank Starmer[a,*], A.O. Grant[b], T.J. Colatsky[c]

[a]*Departments of Biometry/Epidemiology and Medicine (Cardiology), Charleston, SC 29425, USA*
[b]*Department of Medicine (Cardiology), Duke Medical Center, Durham, NC 27710, USA*
[c]*Department of Pharmacology, Medical University of South Carolina, Charleston, SC 29425 USA*

Received 15 July 2002; accepted 4 October 2002

Abstract

Objective: The fate of an impulse arising from stimulation is determined by the ability of the wave front to recruit sufficient Na channels from adjacent cells. Previous numerical studies of mutant Na channels revealed both the velocity of a conditioning wave and the recruiting capacity of the front as determinants of the vulnerable period (VP), an interval within which excitation results in unidirectional conduction. Drugs that block excitatory Na channels in a voltage dependent manner, such as antiarrhythmics, abused substances and antidepressants, slow the restoration of Na conductance trailing an action potential and are associated with proarrhythmia and sudden cardiac death. We hypothesized that drug-induced slowing of Na conductance recovery would flatten the Na conductance restoration gradient thereby reducing the recruiting capacity of a front, extending the VP and increasing the probability of unidirectional propagation. **Methods:** In a cable of ventricular cells, we explored the sensitivity of the VP to voltage-dependent blockade. While varying the unbinding time constant from 100 ms to 5 s, we measured the Na conductance restoration gradient, the liminal length, the refractory period (RP) and the VP. **Results:** Reducing the rate of drug unbinding flattened the restoration gradient, diminished the recruiting capacity of a premature impulse and extended the liminal length, RP and the VP. The VP was linearly dependent on the drug unbinding time constant. Rapidly unbinding drugs (time constant <1 s) reduced the liminal length below that of a quiescent cable. **Conclusions:** Slowing the unbinding rate of voltage-dependent drug block of Na channels extended the RP and the VP. Drugs with unbinding time constants greater than 1 s dramatically increased the probability of unidirectional propagation, reflecting increases in both the RP and the VP. This study provides a new mechanism linking Na channel function, compromised by voltage-dependent Na channel drug block, with proarrhythmic conditions that can lead to sudden cardiac death following premature stimulation.

Keywords: Antiarrhythmic agents; Arrhythmia (mechanisms); Computer modelling; Conduction (block); Impulse formation; Na-channel; Ventricular arrhythmias

1. Introduction

Reentrant arrhythmias arise from disturbances in propagation. The propagation of a wave front in an excitable cable requires that there be a sufficient number of Na^+ ions that can diffuse into adjacent resting cells and raise the membrane potential to the firing threshold. Because Na channels rapidly inactivate, they participate only briefly in wave front expansion and consequently must be replaced with newly recruited channels in order to keep the front from collapsing. The process of charge diffusion, subsequent regional depolarization and opening of Na channels characterizes the recruiting process. The recruiting capacity reflects the density of non-inactivated and unblocked Na channels adjoining the leading edge of the

*Corresponding author. Tel.: +1-843-792-0215; fax: +1-843-792-0258.
E-mail address: starmerf@musc.edu (C.F. Starmer), http://www.musc.edu/~starmerf (C.F. Starmer).

Time for primary review 31 days.

0008-6363/03/$ – see front matter
doi:10.1016/S0008-6363(02)00727-7

front. The fate of an impulse arising from stimulation is thus determined by the ability of the wave front to recruit sufficient Na channels from adjacent cells such that the resulting inward current maintains an active region comparable in size to the liminal length.

When there is an asymmetry in some property essential for propagation, the impulse will evolve in an asymmetric manner and create the potential for unidirectional block and re-entrant proarrhythmia. One source of asymmetry is the conductance restoration gradient that trails a propagating action potential. Recently [1] we demonstrated with numerical studies of a cable of ventricular cells expressing mutant Na channels that slowing recovery from Na channel inactivation flattened the Na conductance restoration gradient and extended the vulnerable period, VP, thus contributing to proarrhythmia. The VP was extended by two mechanisms: a reduction in the propagation velocity of a conditioning wave and a reduction in the recruiting capacity of the wave front. Just as the inactivation gate controls the recovery of resting channel properties during the diastolic interval, voltage dependent drug unblocking during the diastolic interval can alter the density of unblocked channels (recruiting capacity) and thus may exacerbate the same proarrhythmic mechanisms.

A number of reports have associated voltage-dependent Na channel blockade, a property of many antiarrhythmic agents [2–5] and abused substances [6–9], with enhanced proarrhythmia and sudden cardiac death [6,10–17]. Drug-induced alterations in Na channel function and altered inactivation gating induced by genetic mutation are similar and thus may share similar proarrhythmic mechanisms. Here, we extend our studies of altered Na channel function in tissue expressing mutant Na channels with numerical studies of Na channels functionally compromised by voltage-dependent blockade in a cable of identical cells. Similar to altered gating, prolonging the unbinding time constant delayed recovery of Na conductance, extended the refractory period, RP, flattened the Na conductance recovery gradient and prolonged the VP. Extending the VP model from Ref. [1] we derived a linear relationship between the VP and the drug's unbinding time constant, τ_d (inverse unbinding rate). Consequently, knowledge of τ_d derived from kinetic studies of a drug could be used to anticipate alterations in cardiac vulnerability.

2. Methods

We explored impulse formation under conditions producing an asymmetric spatial distribution of Na conductance, g_{Na}, in a one-dimensional cable of homogeneous cardiac cells with reduced maximum Na conductance similar to that reported in Ref. [18]. To reduce confounding influences of multiple currents and facilitate identifying the biophysical mechanisms underlying unidirectional propagation, we used a modified Beeler–Reuter [19] model, replacing the BR Na channel model with the Ebihara–Johnson [20] model. To mimic the compromised conductance reported in [18] we set the maximum Na conductance, G_{Na}, at 10 mS/cm^2, simulating the conductance of ischemic border zone cells. A 5 cm cable was constructed by linking excitable segments ($dx = 1/512$ cm) having an axial resistivity of 250 Ω cm and a cell radius of 7 microns. The discretized equations were solved using an implicit method with a time step of $dt = 1/128$ ms. The boundary conditions at the ends of the cable permitted no current flow ($\partial V/\partial x = 0$).

To locate the VP boundaries, we initiated a conditioning wave (s1) at one end of the cable and, after a short delay, initiated a test wave (s2) at 1.25 cm from one end. The delay was timed to place a test impulse within the Na conductance restoration wave that trailed the s1 front. We probed for the VP boundaries as the Na conductance restoration wave trailing the s1 front passed over the s2 site. The stimulus amplitude and duration of both s1 and s2 stimuli was -62.5 μA/cm^2 and 0.25 ms. The s2 electrode length was equivalent to a point (4/512 cm). We varied the s1–s2 delay and identified the most premature boundary (MPB) as marking the transition from refractory to stable retrograde propagation and the least premature boundary (LPB) as marking the transition to stable bidirectional propagation.

Binding of voltage dependent drugs with the Na channel occurs predominantly during either the channel open interval or while the channel is inactivated. There is minimal binding to channels in the rest state during the diastolic interval. Since the VP occurs during the diastolic interval and the dynamics of Na conductance recovery is dominated by drug unbinding, we limited these studies to variations in the unbinding rate. We set the binding rate, kD, to 0.002/ms, equivalent to 40 μM lidocaine [21]. To explore the role of drug unbinding during the diastolic interval, we varied the unbinding rate from 0.01/ms to 0.0002/ms (the unbinding time constant, τ_d, varied from 100 ms to 5 s). During a train of s1 pulses, each successive s1 wave propagates at a slower velocity than its predecessor until steady-state blockade is achieved. Consequently the study of drug effects on the Na channel per se would be confounded by concomitant changes in s1 velocity. To avoid this confounding factor, we measured the VP following a single conditioning (s1) pulse, thereby minimizing variations in the s1 wave velocity that would be encountered with pulse train stimulation.

For each drug unbinding rate, we measured the refractory period, the vulnerable period, the Na conductance gradient at the VP boundaries, the lifetime of the antegrade front at the least LPB and the liminal length at the LPB. We explored the effect of changes of s2 physical electrode length, L, by varying L from 0.078 (point electrode) to 3.9 mm with kD = 0.002/ms, $l = 0.001$/ms and $G_{Na} = 10$ mS/cm^2.

We estimated the space constant of a quiescent cable by

injecting a subthreshold current of $-0.2\ \mu A/cm^2$ into the middle of the cable for 100 ms, measured the steady-state spatial distribution of membrane potential and then fit an exponential to the profile. We approximated the liminal length [22–26] by first measuring the minimum (0.1% precision) s2 current density (applied for 0.25 ms) required to initiate propagation at the ends of a 5 mm space-clamped segment of cable. We then used that current amplitude and duration to determine the minimum length, L, of the space-clamped region required to initiate stable propagation. The minimum length was estimated by progressively shortening the space-clamped region until removal of 1 dx unit resulted in propagation failure. We measured the liminal length in the middle of a quiescent cable under drug-free conditions. In the presence of drug, we measured the liminal length centered at the s2 site at the time of the LPB of the VP.

The effects of Na channel blockade were modeled according to the guarded receptor paradigm [27] applied to a binding site exposed by channel inactivation. We assumed that receptor accessibility was determined by the inactivated channel conformation. Consequently, the rate of binding depended on the fraction of inactivated channels, $1-h$, where h is the fraction of non-inactivated channels. The binding reaction was described by:

$$U + D(1-h) \underset{l}{\overset{k}{\Leftrightarrow}} B \tag{1}$$

$$\frac{db}{dt} = k[D](1-h)(1-b) - lb \tag{2}$$

where D is the drug concentration, U represents unblocked channels, B represents blocked channels, b is the fraction of blocked channels and k and l are the rates of block and unblock, respectively. The Na current equation was modified to incorporate blockade:

$$I_{Na} = G_{Na} m^3 hj(1-b)(V - V_{Na}) \tag{3}$$

where m is the fraction of activated channels, h and j are the fractions of fast and slow non-inactivated channels, V is the membrane potential and V_{Na} is the sodium reversal potential. The state-dependent Na channel conductance, g_{Na}, was defined by:

$$g_{Na} = G_{Na} hj(1-b) \tag{4}$$

Previously [1], we showed that following the passage of an excitation wave with velocity, v, the VP could be described as the sum of the time required for passage of the threshold for retrograde propagation over the length (L) of the s2 stimulus field and the time required for g_{Na} at the antegrade boundary of the s2 field to exceed the threshold for stable antegrade propagation:

$$VP = \frac{L + \delta / dg_{Na}(x_r)/dx}{v} = \frac{L + L^*}{v} \tag{5}$$

where δ is the difference between the retrograde and antegrade thresholds for propagation and $dg_{Na}(x_r)/dx$ is the gradient of g_{Na} at the most premature boundary of the VP.

When an excitation wave travels with a velocity v, the temporal unbinding at any point can be related to the spatial recovery gradient at that point according to:

$$\frac{\partial g_{Na}}{\partial x} = \frac{\partial g_{Na}}{\partial t}\frac{1}{v} \tag{6}$$

In the presence of drug, the refractory period is prolonged sufficiently to permit full recovery from inactivation. Thus Eq. (4) when applied to the post refractory interval can be simplified to $g_{Na} = G_{Na}(1-b)$. During the post refractory interval, the membrane potential is near the rest potential where unbinding dominates so that the blockade Eq. (2) simplifies to

$$\frac{db}{dt} = -lb \tag{7}$$

From this relationship, the spatial gradient can be computed directly from the unbinding rate according to:

$$\frac{\partial g_{Na}}{\partial x} = -G_{Na}\frac{db}{dt}\frac{1}{v} = G_{Na} l b_{crit}\frac{1}{v} \quad \text{or}$$

$$\frac{\partial g_{Na}}{\partial x} = \frac{G_{Na} b_{crit}}{v\tau_d} \tag{8}$$

where $G_{Na}b_{crit}$ is the conductance threshold for stable retrograde propagation and $\tau_d = 1/l$, the unbinding time constant. Here we see that the recruiting potential in marginally excitable cells is inversely related to both the velocity of the conditioning (s1) wave and the drug unbinding time constant. Thus the VP, in the presence of voltage-dependent Na channel blockade, is described by a relationship that varies linearly with the extent of the s2 stimulus field and drug unbinding time constant and inversely with the s1 velocity and maximum Na conductance:

$$VP = \frac{L}{v} + \frac{\delta\tau_d}{G_{Na} b_{crit}} \tag{9}$$

3. Results

3.1. Responses to stimulation in a quiescent cable

The resting membrane potential for the cable of ischemic border zone cells was -84.5 mV and the threshold G_{Na} for propagation was $5.03\ mS/cm^2$. A small amount of rest inactivation ($h = 0.983$, $j = 0.989$) resulted in a threshold $g_{Na} = 4.89\ mS/cm^2$. The threshold stimulus current density (applied for 0.25 ms) required to establish stable propagation in a quiescent cable with a point electrode (electrode length $= 4dx = 4/512$ cm and $G_{Na} = 10\ mS/cm^2$) was $-7\ \mu A/cm^2$. When the conductance was reduced to the marginally excitable value ($G_{Na} = 5.03\ mS/cm^2$) the threshold current density was $-20\ \mu A/cm^2$. To avoid

altering the stimulus amplitude for different conditions, we set the s2 stimulation current density at -62.5 mA/cm^2, approximately three times that of a marginally excitable cable.

To characterize the recruiting capacity of a wave front, we measured the space constant and space-clamped liminal length, LL, the minimum length of a uniformly excited cable segment necessary to initiate a stable propagating wave. In a quiescent cable, the spatial profile of the membrane potential associated with a subthreshold current was exponential with a space constant of 0.997 mm. The minimum pulse stimulation current density required to establish stable propagation with a 5 mm electrode (exceeding the LL) was -0.750 μA/cm^2 for both $G_{Na}=5.03$ and 10 mS/cm^2. The space-clamped liminal length (LL), using the threshold stimulation current $=0.750$ μA/cm^2 applied for 0.25 ms was 2.66 mm for $G_{Na}=5.03$ mS/cm^2 and 2.65 mm for $G_{Na}=10$ mS/cm^2.

3.2. Responses to stimulation in the wake of a conditioning wave

Shown in Fig. 1 are the responses for the s1–s2 delays associated with the most (MPB) and least (LPB) premature boundaries of the VP. Panels A–D depict responses for

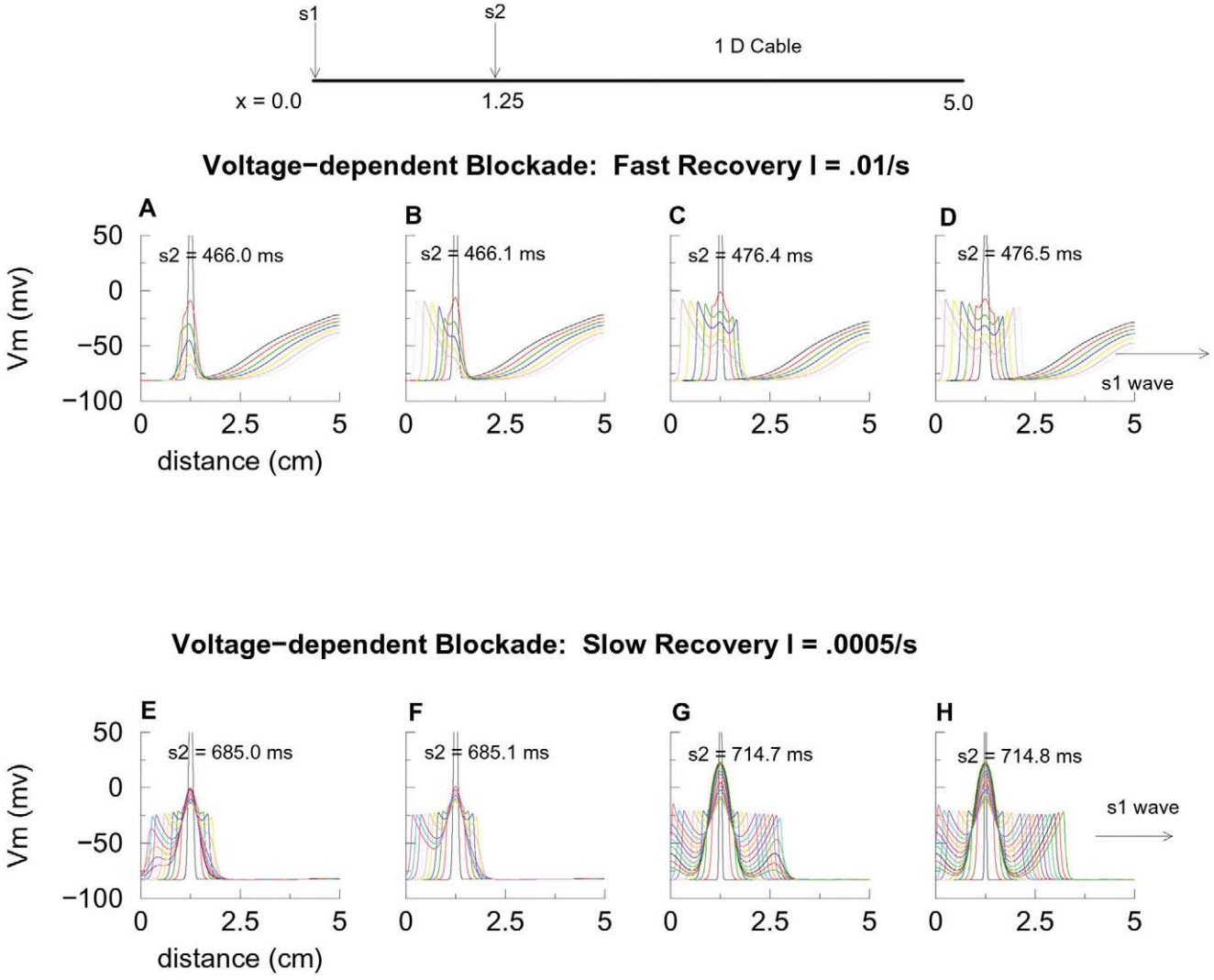

Fig. 1. The boundaries of the vulnerable period as determined by the range of s1–s2 delays resulting in unidirectional propagation. The black trace represents the first post-stimulus potential profile. Each color (red, green, blue ...) depicts a snapshot (taken every 5 ms after the s2 stimulus) of the spatial membrane potential. Shown here are two conditions: the responses at the MPB (panels A, B) and LPB (panels C, D) for a rapidly unbinding ($l=0.01$/s) voltage-dependent drug and the responses at the MPB (panels E, F) and LPB (panels G, H) for a slowly unbinding ($l=0.0005$/s) voltage-dependent drug. Note the rapid collapse of both the retrograde front (panel A) and antegrade front (panel C) for the rapidly unbinding drug compared with the slower retrograde collapse (panel E) and antegrade collapse (panel G) associated with a slowly unbinding drug. The increased lifetime of decremental propagation of the antegrade impulse (panel G) is the result of the marginal recruiting capacity associated with a nearly flat conductance restoration gradient when the Na conductance is marginal (see Fig. 2) compared with the lifetime of decremental propagation of the antegrade impulse (panel C) in the presence of the rapidly unbinding agent.

a rapidly unbinding drug (unbinding rate = 0.01/s; $\tau_d = 100$ ms) while panels E–H depict responses for a slowly unbinding drug (unbinding rate of 0.0005/s; $\tau_d = 2$ s). The potential profiles were plotted at 5 ms intervals after the stimulus. Panels A, B and E, F show the transition from block to stable retrograde propagation at the most premature boundary while panels C, D and G, H show the transition to stable antegrade propagation at the least premature boundary. Reducing τ_d from 100 ms to 2 s increased the VP almost three-fold from 10.3 to 29.5 ms while the s1 wave velocity was essentially constant (44.1 and 42.7 cm/s, respectively). The dynamics of antegrade front collapse (panels C and G) was quite different, collapsing after 20 ms of decremental propagation when $l = 0.01$/s but requiring approximately 70 ms of decremental propagation before collapse when $l = 0.0005$/s. Shown in Table 1 are the detailed measurements of the VP boundaries, s1 velocities, the conductance restoration gradient at the MPB, the liminal length measured at the LPB and the lifetime of the antegrade wave at the LPB.

3.3. Altered Na conductance restoration and na channel recruiting

Previously, we demonstrated that the MPB and LPB of the VP coincided with a g_{Na} threshold for stable retrograde propagation and a larger threshold for stable antegrade propagation [1]. In these studies we observed that as τ_d was prolonged, the restoration Na conductance spatial profile was flattened and approached a constant value similar to that of a quiescent cable. Since the threshold of excitation in a quiescent cable was less than either the antegrade or retrograde thresholds observed during drug-free conditions [1], we hypothesized that as τ_d was increased, the thresholds of retrograde and antegrade propagation would decline slightly, thereby smearing the collocation of thresholds observed in Ref. [1, Fig. 2]. To test this idea, we plotted the spatial distribution of Na channel conductance ($g_{Na}hj(1-b)$) at the s1–s2 delays associated with the MPB and LPB of the VP (Fig. 2). In contrast to the well defined retrograde intersections of g_{Na} profiles associated with rapid restoration of Na conductance [1, Fig. 2A, $5.02 < g_{Na} < 5.07$], panel A shows a less well defined intersection of conductance profiles for τ_d less than 1 s and significant departure from the threshold for $\tau_d > 1$ s ($4.94 < g_{Na} < 5.04$). The average MPB conductance threshold was 4.99 mS/cm^2 while the average LPB conductance threshold was 5.13 mS/cm^2, both of which were less than the drug-free thresholds observed in Ref. [1]. Similarly as seen in panel B, the antegrade threshold was less well defined ($4.98 < g_{Na} < 5.17$) when compared with Ref. [1, Fig. 2B, ($5.20 < g_{Na} < 5.26$] and here also, the dispersion increased as τ_d was prolonged.

We next explored the relationship between the VP and length of the stimulus electrode (Fig. 3). According to the VP model of Wiener and Rosenbleuth (WR) [28], the VP should vary linearly with the length of the suprathreshold region of the s2 stimulus field. Fig. 3 shows the results of determining the VP in a cable with $G_{Na} = 10$ mS/cm^2 at lengths of 0.078, 0.39, 0.78, 1.56, 2.34, 3.12 and 3.9 mm. For lengths less than the liminal length (2.6 mm) the measured VP was less than that predicted by the WR model ($VP = L/.v$). However for lengths greater than the LL, the VP was accurately predicted by a linear relationship ($r = 0.99$) with an intercept of 35.6 ms and a slope of 24.9 ms/cm. According to the WR model, the slope is determined by the inverse s1 velocity. The reciprocal slope was 40.2 cm/s which was in close agreement with the observed s1 wave velocity of 43.5 cm/s.

3.4. Measures of anti- and proarrhythmic potential

We explored the link between antiarrhythmic and proarrhythmic potential with plots (Fig. 4) of the RP, (panel A), VP (panel B), the probability of unidirectional propagation, prob(UP), (panel C) and the liminal length (panel D) as a function of τ_d. We estimated the prob(UP), by assuming a heart rate of 75 (800 ms interval) and then computed the probability of UP as the ratio of the VP to the excitable interval: $p(UP) = VP/(RR - RP)$ where RR is the R–R interval. Increases in τ_d increased both the RP (panel A) and the VP (panel B). The prob(UP) increased dramatically for $\tau > 1$ s. For $\tau > 2$ s, measurements of prob(UP) were not possible since the refractory period

Table 1
Vulnerable period measurements: variations in drug unbinding rate

Unbinding rate (/s)	RP (ms)	VP (ms)	S1 velocity (cm/s)	$dg_{Na}(MPB)/dx$ mS/cm^2/cm	Liminal length (mm)	Antegrade life (ms)
0.0002	1553.6	46.9	40.599	−0.00281	2.66*	110
0.0003	990.2	37.1	41.574	−0.00358	2.64**	90
0.0005	685.1	29.5	42.712	−0.00486	2.38	70
0.0007	582.0	23.1	43.127	−0.00794	2.25	60
0.001	517.7	20.7	43.455	−0.02739	2.07	50
0.002	484.6	13.7	43.824	−0.11034	2.01	30
0.005	470.6	11.1	44.053	−0.24858	1.91	25
0.01	466.1	10.3	44.114	−0.34714	1.84	20
0.0 (control)	462.6	9.7	44.21	−0.44518	2.66	10

* $I(s2) = 0.000770$ mA/cm^2; ** $I(s2) = 0.000764$ mA/cm^2; otherwise $I(s2) = 0.000750$ mA/cm^2).

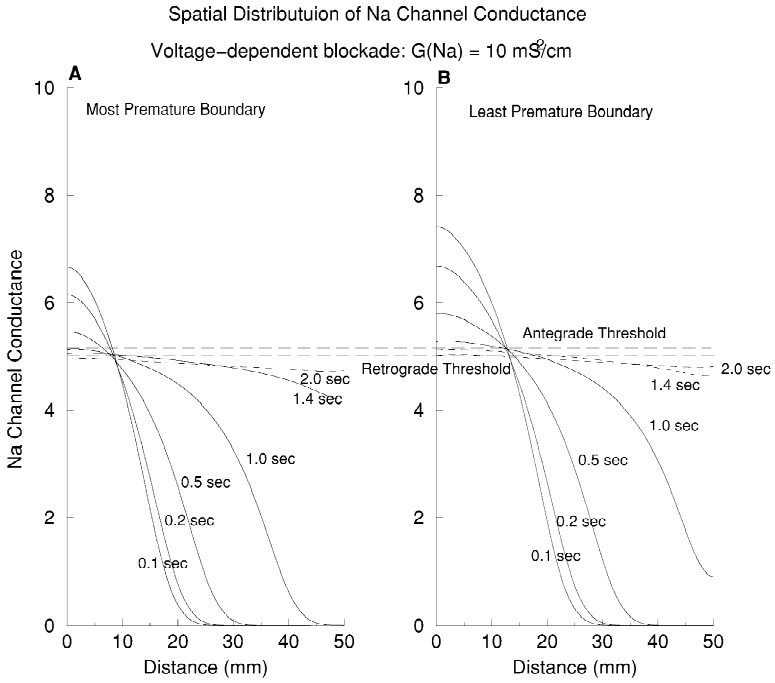

Fig. 2. Spatial restoration profiles of Na channel conductance: $g_{Na} = G_{Na} hj(1 - b)$, at the s1–s2 delay associated with the MPB (panel A) and the LPB, of the VP (panel B). Alignment of the conductance profiles revealed a region of intersections that defined the threshold of retrograde and antegrade propagation for $\tau_d < 1$s. As τ_d increased, the restoration profiles fell below these intersections, implying a smaller threshold for stable propagation as the restoration gradient approached zero and consistent with the uniform excitability of a quiescent cable.

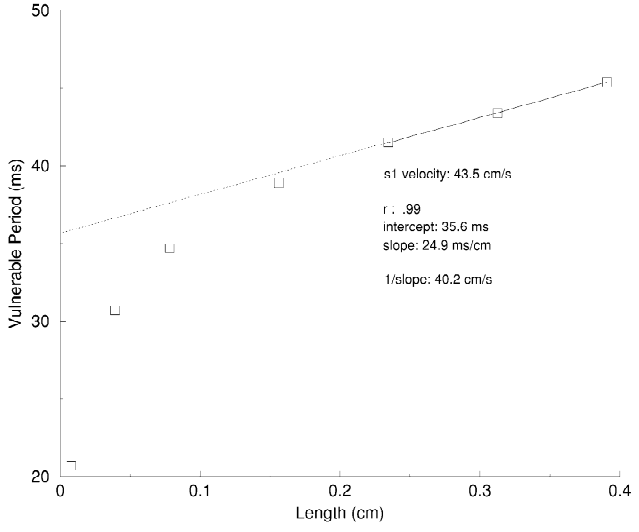

Fig. 3. The dependence of the VP on the electrode length in the presence of a voltage-dependent drug (kD = 0.002/s and 1 = 0.001/s). The liminal length was 2.07 mm. For lengths greater than the liminal length, the relationship between the VP and length agreed with Eq. (9), ($r = 0.99$). The least squares estimate of the slope was 24.9 ms/cm. Testing the agreement between the mechanistic basis of Eq. (9), we computed the estimated velocity from the reciprocal slope as 40.2 cm/s, in close agreement with the observed s1 velocity of 43.5 cm/s. For lengths less than the liminal length, the VP was underestimated, due to shortening of the s2 stimulus field by the liminal length requirement.

exceeded 800 ms, the excitation interval. From the plot (panel B) of VP against τ_d, we tested the linear relationship predicted by Eq. (9). Because we used only a single s1 pulse, the s1 wave velocity was comparable (see Table 1) for all conditions, thus L/v should be constant while the second term should vary with τ_d. Panel B shows the predicted linear relationship ($r = 0.99$). Panel D illustrates the changes in the liminal length as τ_d was increased. It is interesting to note that when $\tau_d < 3$ s, the space-clamped liminal length at the VP boundary was less than that for a quiescent medium.

3.5. Characterizing Na channel recruiting

Previously [1], we identified Na channel recruiting as a major determinant of whether an impulse would propagate or collapse. We viewed Na channel recruiting as the process of diffusion of charge carriers down a potential and concentration gradient from the wave front into adjoining cells. We hypothesized that the space constant would govern the effective recruiting range of the front while the spatial gradient of recovered Na channels would determine the recruiting capacity, the density of recruited non-inactivated and unblocked Na channels per space constant. To better understand recruiting, we measured the space constant (Fig. 5A) and explored the relationship between the restoration gradient and steady-state velocity under drug-free conditions (Fig. 5B). Shown here is the restoration gradient at the most premature boundary (the

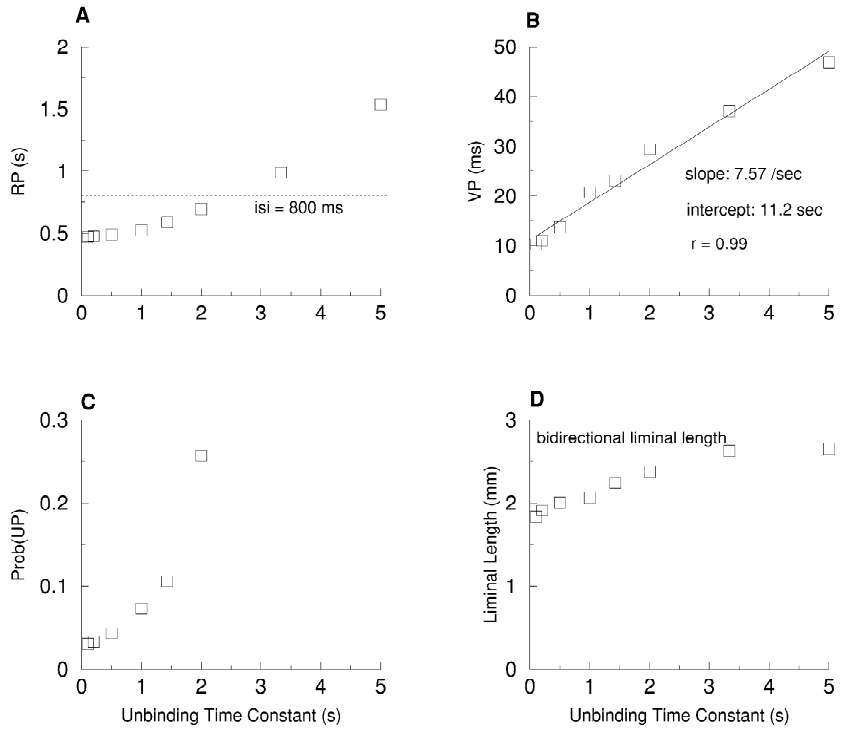

Fig. 4. The unbinding time constant alters the refractory period (RP, panel A), the vulnerable period (VP, panel B) and the probability of unidirectional propagation. (Prob (UP), panel C) and the space-clamped liminal length (panel D). All parameters increased as τ_d decreased. The VP relationship with τ_d was linear ($r = 0.99$) as predicted by Eq. (9) since the s1 conditioning velocity was virtually unchanged over the range of unblocking time constants. Similarly, the liminal length increased as τ_d increased, and reached a limiting value of 2.66 mm, equal to the liminal length of a quiescent cable. Because the refractory period extended beyond 800 ms, the probability of unidirectional propagation, prob(UP), could not be estimated (since the cycle length was 800 ms). Not that as τ_d increased the probability of UP increased dramatically, signaling both the reduction in the excitable interval as the RP increased and the increase in the VP.

transition from block to stable retrograde propagation) of the VP plotted against the s1 conduction velocity (from Table 1 in Ref. [1]). The resulting linear relationship suggests that the Na conductance and its gradient measured at the threshold for propagation influence propagation and can be used as a measure of a wave front's recruiting capacity. Furthermore, it is interesting to note that the measured space-clamped liminal lengths (Table 1) all fall within three space constants, consistent with using the space constant as a measure of the spatial extent of the recruiting process.

Summarizing the results, the extent of recruiting de-

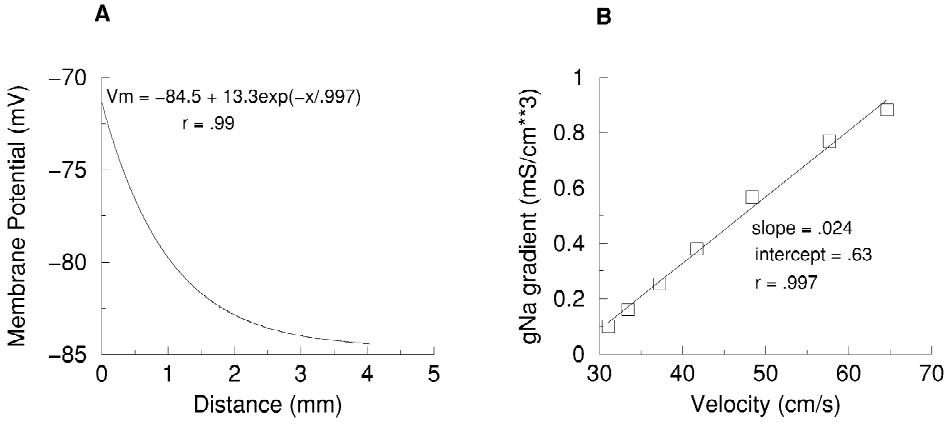

Fig. 5. Panel A. The spatial potential distribution associated with subthreshold stimulation. The potential distribution was accurately fit with a single exponential with a space constant of 0.997 mm. Panel B. The relationship between the Na conductance restoration gradient and steady-state velocity in a drug free cable. The points represent the conductance gradients measured at the most premature boundary of the VP for G_{Na} values ranging from 6.0 to 24.25 mS/cm^2. The relationship was well fit by a straight line.

pends on the space constant and the capacity depends on the spatial distribution of Na conductance. Slowing the unbinding rate (prolonging the unbinding time constant) of voltage-dependent Na channel blockers flattens the Na conductance restoration gradient, increases the liminal length and extends the VP. Interestingly, accelerating unbinding reduced the minimum excited region necessary to establish stable propagation. As in Ref. [1] we observed thresholds for stable retrograde and antegrade propagation, though the intersections of conductance profiles were more diffuse than seen in the drug-free conditions. Finally, the VP was linearly related to τ_d of voltage-dependent Na channel blockers and to the length of the s2 electrode for lengths greater than the liminal length.

4. Discussion

A front, successfully expanding in tissue, requires recruiting an adequate supply of charge carriers (e.g. Na^+) that can diffuse down a concentration and voltage gradient into adjacent resting cells thereby depolarizing the local membrane potential to the Na channel opening threshold. Because recently recruited Na channels inactivate, they must be rapidly replaced with newly recruited channels in order to prevent front collapse. We refer to the process of charge diffusion and subsequent opening of resting Na channels adjacent to the front as a recruiting process. The amount of recruited charge, as determined by the recruiting range and the restored Na conductance density within this range, are critical determinants of not only whether propagation can be sustained but also the propagation velocity.

The supply of replacement charge carriers arises from Na channels residing within a potential liminal region [22–26] adjoining the front. Propagation succeeds when the recruited Na channel density within the potential liminal region (and available charge carriers) in the direction of propagation exceeds a threshold and fails when the recruited Na channel density falls below this threshold. When Na conductance is uniform, as in a resting cable, an impulse larger than the liminal length will propagate in both directions if the conductance is greater than the threshold g_{Na}. That the space-clamped liminal region falls within three space constants suggests that the determinants of the resting cellular membrane resistance (perhaps dominated by the K+ inward rectifier conductance) plays a critical role in defining the recruiting range of the wave front.

Only when there is an asymmetry in some property essential for propagation (e.g. internal resistance, cell diameter, Na conductance, anisotropic cellular connectivity) will the impulse evolve in an asymmetric manner (e.g. unidirectional propagation). One source of this essential asymmetry is the conductance restoration wave that trails a propagating action potential. Within the conductance restoration wave is a critical conductance that separates excitable from refractory cells and the interaction of this boundary with a field of stimulus current creates a vulnerable region. Because there is a threshold for retrograde propagation (Fig. 2A and Fig. 2A in Ref. [1]), the restoration gradient at the threshold g_{Na} can be used to compute the density of recruitable channels per space constant and estimate the VP. Thus interventions that alter the restoration gradient (altered channel gating, voltage-dependent blockade, a prior premature excitation) or the space constant and liminal length can be evaluated in terms of their predicted effect on the VP. Moreover, using the relationship between time and spatial derivatives, we showed that the VP was directly proportional to τ_d and observed that drugs with long unbinding time constants (>1 s) were associated with much higher probabilities of unidirectional conduction than drugs with short unbinding time constants (<1 s).

Liminal length estimates in earlier investigations [22,23,25] were based on point stimulation and ranged from 0.2 to 0.5 space constants which is significantly shorter than our space-clamped measurement. These earlier estimates were based on strength-duration curves and a steady-state analysis of the spatial distribution of membrane currents. With a non-inactivating source of inward current, a spatial balance of the inward and outward currents along the length of cable resulted in a stationary wave (zero velocity) where the spatial profile of membrane potential was approximately Gaussian [29]. Within this context the liminal length for point stimulation was comparable to the standard deviation of the Gaussian wave. Our measurements, based on uniform excitation of a minimal segment of space-clamped cable resulted in liminal lengths between two and three space constants, reflecting the distance required for collapse from an activated space-clamped region to a pulse similar to the Gaussian pulses described above. The longer estimates of the liminal length in our study reflect the difference between the non-steady-state responses to uniform depolarization and responses to non-uniform point depolarization. Both perspectives are important for understanding mechanisms of propagation.

We found the liminal region to be sensitive to the drug unbinding time constant. We hypothesize that in a quiescent cable, a liminal length of excited cable feeds two fronts while in the presence of a gradient of Na conductance, the disposition of charge carriers within the liminal region depends on the gradient of recruited channels. Drug unbinding created a gradient in Na conductance within the vulnerable region that altered the antegrade and retrograde recruiting potential. When τ_d was short, the liminal length was significantly shorter than the quiescent liminal length (2.66 mm), possibly a result of having to ignite only a single (retrograde) front. However, as τ_d increased, the conductance profile flattened (Fig. 2) and approached that of a quiescent cable with uniform conductance. With

smaller Na conductance gradients, the likelihood of successful antegrade propagation at the LPB of the VP increased, as reflected by an increase in the liminal length which asymptotically approached that of the quiescent length.

We found the VP to be sensitive to the electrode length. When the length of the s2 stimulation electrode was greater than the liminal length, then the VP increased in proportion of the electrode length, in agreement with the WR model [28]. However, when the length was less than the liminal length, the VP was disproportionately shorter, indicative that the combined length of the excitation field and the physical electrode did not meet the liminal requirements for propagation until the threshold for retrograde propagation had passed some distance over the physical electrode. Said another way, the stimulus pulse from a point source alone, was inadequate to excite a liminal region and thus the MPB of the VP was delayed until enough of the physical electrode was available to increase the excited region to the liminal threshold.

Reports of sudden cardiac death are often associated with the use of a voltage-dependent Na channel blocking agent. For example, the CAST study [2], designed to test the efficacy of PVC suppression with slowly unbinding voltage-dependent Na channel blockade, graphically demonstrated that the residual unsuppressed PVCs, by some mechanism, resulted in an increase of sudden cardiac death. The drugs used in CAST all had unbinding recovery times greater than 1 s [30] and our analysis indicates that RP and VP extension secondary to slowed recovery of availability will increase the probability that an unsuppressed PVC can initiate unidirectional propagation.

Similar to the CAST report, we observed an association between emergency room admissions with ventricular tachyarrhythmias and substance abuse [6]. Cellular studies revealed that propoxyphene [6], cocaine [7] and some tricyclic antidepressants [8] all blocked the cardiac sodium channel in a voltage-dependent manner and all exhibited unbinding time constants in excess of 5 s. The Na channel blocking properties of cocaine used as a recreational drug was suggested as the proarrhythmic agent leading to sudden cardiac death in young healthy individuals [15]. In addition, a population-based study from Olmstead county [16] reported a high prevalence of cocaine abuse in young adults who died suddenly. Ketamine had also been shown to block neuronal Na channels [9,31] and has been linked with tachycardia among substance abusers [17]. In vitro studies of Na channel blockade [10,11] strengthen the link between voltage dependent blockade and VP extension. In these studies lidocaine, a short recovery time constant agent, produced a much smaller extension of the VP than the longer recovery time constant agents (flecainide, cocaine and propoxyphene), consistent with the proarrhythmic mechanisms identified here.

With voltage-dependent blockade, we observed that the thresholds for stable retrograde and antegrade propagation were not collocated as distinctly as observed in Ref. [1]. As τ_d increased beyond 1 s, the restoration gradient became flatter, approaching that of a uniformly excitable cable (as if only G_{Na} were reduced) and the threshold for retrograde propagation fell below the threshold observed in Ref. [1]. For a quiescent, uniformly excitable cable, the recruiting capacity was directionally symmetric. With a gradient of excitability trailing the s1 wave, the recruiting capacity was greater in the retrograde direction than in the antegrade direction. However, as τ_d increased, the restoration gradient approached that of a uniformly excitable cable where the g_{Na} recruiting profile was almost symmetric. The result was that the threshold for retrograde propagation was actually lower than that observed in the presence of a large gradient.

Extending our results to three-dimensional tissue characterized by anisotropic connectivity, non-uniform cellular refractory properties and variations in ionic gradients is uncertain. However we have tried to facilitate extrapolation by focusing our investigations on a generic proarrhythmic mechanism, the vulnerable period, an interval that exists in simple, homogeneous, excitable chemical and biological preparations and which cannot be suppressed by added complexities. Furthermore, our approach is based on mechanisms that can be derived from basic biophysical concepts. For characterizing ventricular cells, we have used cable theory with the Beeler–Reuter cellular model [19] and the Ebihara–Johnson [20] Na channel model. We have used the guarded-receptor paradigm of voltage-dependent blockade [27], a physical model that has been validated in our laboratory [21] and the laboratories of others [32,33]. We have focused on the vulnerable period, a generic property of all excitable systems [26,28,34,35] and identified important determinants of vulnerability that are applicable to three dimensional tissue.

The VP is a possible common denominator linking many clinical reports of proarrhythmia, associated with antiarrhythmic agents [2,13], cocaine [15,16] and other abused substances [6,17]. It is important to realize that vulnerability exists in any homogeneous excitable medium and does not require variations of cellular refractory properties. The principles explored in this study thus provide a minimally complex mechanistic substrate for probing the sensitivity of proarrhythmic processes to a number of clinically meaningful conditions and provides a basis for exploring the modulating influences of structural complexities and non-uniform cellular properties in multidimensional preparations.

Use-dependent channel blockade is derived from the voltage sensitivity of the drug-channel interactions. Utilizing the mathematical link between spatial and temporal derivatives, we were able to show that the VP was directly proportional to the drug unbinding time constant. Slowly unbinding drugs such as flecainide, cocaine, propoxyphene and amitriptylene dramatically increased both the RP and the VP compared with rapidly unbinding drugs such as

lidocaine. Thus, with voltage-dependent blockade, the probability of unidirectional propagation is disproportionately amplified because both he VP and the RP increase. These relationships should prove useful in the evaluation of potential antiarrhythmic agents and future investigations of proarrhythmic mechanisms.

References

[1] Starmer CF, Colatsky TJ, Grant AO. What happens when cardiac Na channels lose their function? 1: Numerical studies of the vulnerable period in tissue expressing mutant channels. Cardiov Res 2003;57:82–91.

[2] The Cardiac Arrhythmia Suppression Trial (CAST) investigators. Preliminary report: effect of encainide and flecainide on mortality in a randomized trial of arrhythmia suppression after myocardial infarction. New Engl J Med 1989;432:406–412.

[3] Johnson EA, McKinnon MG. The differential effect of quinidine and pyralamine on the myocardial action potential at various rates of stimulation. J Pharmacol Exp Ther 1957;120:460–468.

[4] Heistracher P. Elektrophysiologische untersuchungen über den mechanismus der wirkung eines antifibrillans auf de anstiegssteilheit des aktionspotentials von Purkinje-fasern. Pflugers Arch 1964;279:305–329.

[5] Heistracher P. Mechanism of action of antifibrillatory drugs. Naunyn Schmeideberg Arch Pharmacol 1971;269:199–212.

[6] Whitcomb DC, Gilliam FR, Starmer CF, Grant AO. Marked QRS complex abnormalities and sodium channel blockade by propoxyphene reversed by lidocaine. J Clin Invest 1989;84:1629–1636.

[7] Crumb WJ, Clarkson CW. Characterization of cocaine-induced block of cardiac sodium channels. Biophys J 1990;57:589–599.

[8] Barber JM, Starmer CF, Grant AO. Blockade of cardiac sodium channels by amitriptyline and diphenylhydantoin: evidence of two voltage-dependent binding sites. Circ Res 1991;69:677–696.

[9] Brau ME, Sander F, Vogel W, Hempelmann G. Blocking mechanisms of ketamine and its enantiomers in enzymatically demyelinated peripheral nerve as revealed by single-channel experiments. Anesthesiology 1997;86:394–404.

[10] Starmer CF, Lancaster AR, Lastra AA, Grant AO. Cardiac instability amplified by use-dependent Na channel blockade. Am J Physiol 1992;262:H1305–1310.

[11] Nesterenko VV, Lastra AA, Rosenshtraukh LV, Starmer CF. A proarrhythmic response to sodium channel blockade: modulation of the vulnerable period in guinea pig ventricular myocardium. J Cardiov Pharm 1992;19:810–820.

[12] Krishnan SC, Josephson ME. ST segment elevation induced by class IC antiarrhythmic agents: underlying electrophysiologic mechanisms and insights into drug-induced proarrhythmia. J Cardiovasc Electrophysiol 1998;11:1167–1172.

[13] Herre JM, Titus C, Oeff M, Eldar M, Franz MR, Griffin JC, Scheinman MM. Inefficacy and proarrhythmic effects of flecainide and encainide for sustained ventricular tachycardia and ventricular fibrillation. Ann Intern Med 1990;113:671–676.

[14] Nattel S. The molecular and ionic specificity of antiarrhythmic drug actions. J Cardiovasc Electrophysiol 1999;10:272–282.

[15] Bauman JL, Grawe JJ, Winecoff AP, Hariman RJ. Cocaine-related sudden cardiac death: a hypothesis correlating basic science and clinical observations. J Clin Pharmacol 1994;34:902–911.

[16] Shen W, Edwards WD, Hammill SC, Bailey KR, Ballard DJ, Gersh BJ. Sudden unexpected nontraumatic death in 54 young adults: a 30 year population-based study. Am J Cardiol 1995;76:148–152.

[17] Weiner AL, Vieira L, McKay CA, Bayer MJ. Ketamine abusers presenting to the emergency department: a case series. J Emerg Med 2000;18:447–451.

[18] Pu J, Boyden PA. Alterations of Na+ currents in myocytes from epicardial border zone of the infracted heart: a possible ionic mechanism for reduced excitability and postrepolarization refractoriness. Circ Res 1997;81:110–119.

[19] Beeler GW, Reuter H. Reconstruction of the action potential of ventricular myocardial fibers. J Physiol 1977;268:177–210.

[20] Ebijara L, Johnson EA. Fast sodium current in cardiac muscle: A quantitative description. Biophys J 1980:779–790.

[21] Gilliam FR, Starmer CF, Grant AO. Blockade of rabbit atrial sodium channels by lidocaine: Characterization of continuous and frequency-dependent blocking. Circulation 1989;65:723–739.

[22] Rushton WAH. Initiation of the propagated disturbance. Proc R Soc B 1937;124:210–243.

[23] Fozzard HA, Schoenberg M. Strength-duration curves in cardiac Purkinje fibres: effects of liminal length and charge distrubution. J Physiol 1972;226:593–618.

[24] Noble D, Stein RB. The threshold conditions for initiation of action potentials by excitable cells. J Physiol 1966;187:129–162.

[25] Noble D. The relation of Rushton's liminal length for excitation to the resting and active conductances of excitable cells. J Physiol 1972;226:573–591.

[26] Starobin J, Zilberter YI, Starmer CF. Vulnerability in one-dimensional excitable media. Physica D 1994;70:321–341.

[27] Starmer CF, Grant AO. Phasic ion channel blockade: a kinetic model and method for parameter estimation. Mol Pharmacol 1985;28:348–356.

[28] Wiener N, Rosenblueth A. The mathematical formulation of the problem of conduction of impulses in a network of connected excitable elements, specifically in cardiac muscle. Arch Inst Cardiol Mex 1946;16:205–265.

[29] Neu JC, Preissig RS, Krassowska W. Initiation of propagation in a one-dimensional excitable medium. Physica D 1997;102:285–299.

[30] Weirich J, Antoni H. Differential analysis of the frequency-dependent effects of class 1 antiarrhythmic drugs according the periodical ligand binding: Implications for antiarrhythmic and proarrhythmic efficacy. J Cardiovasc Pharm 1990;15:998–1009.

[31] Irnaten M, Wang J, Chang KS, Andresen MC, Mendelowitz D. Ketamine inhibits sodium currents in identified cardiac parasympathetic neurons in nucleus ambiguous. Anesthesiology 2002;96:659–666.

[32] Valenzuela C, Snyders DJ, Bennett PB, Tamargo J, Hondeghem LM. Stereoselective block of cardiac sodium channels by bupivacaine in guinea pig ventricular myocytes. Circulation 1995;92:3014–3024.

[33] Bou-Abboud E, Nattel S. Molecular mechanisms of the reversal of imipramine-induced sodium channel blockade by alkalinization in human cardiac myocytes. Card Res 1998;38:395–404.

[34] Starmer CF, Lastra AA, Nesterenko VV, Grant AO. Proarrhythmic response to sodium channel blockade: theoretical model and numerical experiments. Circulation 1991;84:1364–1377.

[35] Starmer CF, Biktashev VN, Romashko DN, Stepanov MR, Makarova ON, Krinsky VI. Vulnerability in an excitable medium: analytical and numerical studies of initiating unidirectional propagation. Biophys J 1993;65:1775–1787.